

# Interaction between physical and chemical weathering of argillaceous rocks and the effects on the occurrence of acid mine drainage (AMD)

Matsumoto, Shinji

Department of Earth Resources Engineering, Faculty of Engineering, Kyushu University

Shimada, Hideki

Department of Earth Resources Engineering, Faculty of Engineering, Kyushu University :  
Professor

Sasaoka, Takashi

Department of Earth Resources Engineering, Faculty of Engineering, Kyushu University :  
Associate Professor

<https://hdl.handle.net/2324/4355477>

---

出版情報 : Geosciences Journal. 21 (3), pp.397-406, 2017-05-09. Springer Nature  
バージョン :  
権利関係 :



**Interaction between physical and chemical weathering of argillaceous rocks and  
the effects on the occurrence of acid mine drainage (AMD)**

Shinji Matsumoto<sup>1\*</sup>, Hideki Shimada<sup>1</sup>, Takashi Sasaoka<sup>1</sup>

1. Department of Earth Resources Engineering, Kyushu University, Fukuoka, Nishiku,  
Motoooka 744, Japan

Shinji Matsumoto<sup>1\*</sup>, e-mail: shinji12@kyudai.jp

Hideki Shimada<sup>1</sup>, e-mail: shimada@mine.kyushu-u.ac.jp

Takashi Sasaoka<sup>1</sup>, e-mail: sasaoka@mine.kyushu-u.ac.jp

Short running title:

**Interaction between physical and chemical weathering of argillaceous rocks**

---

\* Corresponding author: shinji12@kyudai.jp  
Tel: +81928023334; Fax: +81928023368

**Abstract:** The disintegration of rocks by weathering plays an important role in the occurrence of Acid Mine Drainage (AMD), which is the environmental problem caused by the exposure of sulfide minerals to water and oxygen. The weathering of rocks is, generally, classified into physical or chemical weathering. However, there are few studies that focus on the complex interaction between physical and chemical weathering of rocks and on the effects of the interaction on the occurrence of AMD. This paper elucidates the complex interrelation between physical and chemical weathering of rocks as well as the progress of AMD through leaching test and weathering test with argillaceous rocks taken in open-cast coal mine in Indonesia in addition to sample analysis before and after the wetting and drying cycle: the rock samples were exposed to oxygen and water during the cycle. The results indicated that the argillaceous rocks which consist of sulfide and/or sulfate caused chemical weathering with micro-cracks on the surface of rocks through the dissolution of soluble iron and sulfur during the occurrence of AMD. Additionally, physical weathering of rocks due to clay minerals was accelerated by chemical weathering with the development of cracks with the occurrence of AMD in the argillaceous rocks containing kaolinite and pyrite. Although weathering of rocks also accelerated AMD, it was concluded that

35 the sulfur content, the form of sulfur and iron in rocks, and the supply of oxygen

36 significantly contributed to the occurrence of AMD.

37

38 **Keywords:** Acid Mine Drainage (AMD), physical weathering, chemical

39 weathering, argillaceous rocks

40

41

42

43

44

45

46

47

48

49

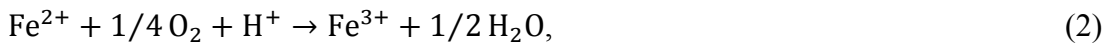
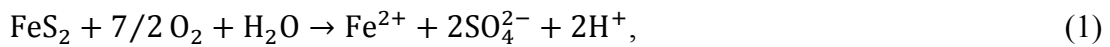
50

51

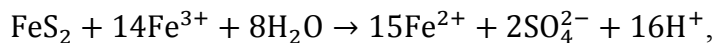
52

## 1. INTRODUCTION

Acid Mine Drainage (AMD), which is the environmental problem caused by the exposure of sulfide minerals to water and oxygen, has a negative impact on the ecosystem in the surrounding area owing to low-pH and heavy metals dissolved with the decrease of pH (Jennings et al., 2008). It is mainly caused by the oxidation of pyrite, and the main oxidants are  $O_2$  and  $Fe^{3+}$  as shown in Eq. (1) and Eq. (3). Firstly,  $Fe^{2+}$  is dissolved from pyrite (Eq. (1)), and  $Fe^{2+}$  is oxidized to  $Fe^{3+}$  by  $O_2$  (Eq. (2)).



With the reaction progress as presented above, the pH decreases. The oxidation of pyrite is, moreover, accelerated by  $Fe^{3+}$  which is strong oxidant (Eq. (3)). Depending on pH,  $Fe^{3+}$  precipitates as  $Fe(OH)_3$  (Eq. (4)).



(3)



71

72 To carry out effective measures against AMD, it is necessary to elucidate the  
73 mechanism and the cause of AMD. The weathering of rocks is one of the key factors for  
74 understanding the progress of AMD in nature since the weathering of rocks easily  
75 occurs under acid conditions, and it causes the release of most of the elements (Jennings  
76 et al., 2008; Dold et al., 2013). The weathering of rocks is classified into physical or  
77 chemical weathering by the types of the cause of the weathering such as rain, snow,  
78 wind and temperature, resulting in a complex mechanism of the progress of the  
79 weathering of rocks (Lobb and Femmer, 2007; Moon and Jayawardane, 2004). Since  
80 the weathering of rocks can affect the occurrence of AMD through the increase of  
81 reactive area of rocks with the disintegration, the progress of AMD has to be  
82 investigated in terms of physical and chemical weathering of rocks. However, there are  
83 few studies that focus on the complex interaction between physical and chemical  
84 weathering of rocks and the effects of the interaction on the occurrence of AMD.

85 In this study, leaching test and weathering test were conducted with argillaceous rock  
86 which is a sedimentary rock formed by clay and taken in open-cast coal mine in  
87 Indonesia in addition to sample analysis before and after the wetting and drying cycle:  
88 the rock samples were exposed to oxygen and water during the cycle.. On the basis of

the results, we examined the interaction between physical and chemical weathering of rocks as well as the effect of the interaction on AMD.

## 2. MATERIALS AND METHODS

### 2.1. Rock Samples and Analytical Methods

Rock samples were collected in pit in the coal mine in Indonesia where the weathering of rocks and the occurrence of AMD have been reported owing to heavy rain and high temperature in the tropical climate. Four samples which were not exposed to the atmosphere were taken from the wall in pit, followed by sample analysis in a laboratory. All samples were categorized as argillaceous rock according to geological data in the mine. They were named as sample A, B, C, and D, respectively. These samples were dried at 50°C in a nitrogen atmosphere for 24 hours to supply for X-ray Diffraction (XRD) and X-ray Fluorescence (XRF) analysis. Major minerals in the samples were analyzed using the X-ray diffractometer (Rigaku, Ultima IV, Japan) under the following condition: radiation CuK $\alpha$ , operating voltage 40 kV, current 26 mA, divergence slid 1 deg, anti-scatter 1deg, receiving slit 0.3 mm, step scanning 0.050°, scan speed 2.000°/min, scan range 2.000-65.000°. In addition, quartz index (QI) was calculated based on the results of XRD analysis in order to compare the mineral content

of the samples. QI was calculated by dividing the maximum intensity ( $I_m$ ) of the target mineral in the sample by X-ray intensity of 100 wt% of standard quartz ( $I_p$ ) which was measured under the same conditions as follows (Okawara et al., 1996):

$$QI = I_m/I_p \times 100$$

Whereas QI is affected by the effect of X-ray mass-absorption coefficient and the difference of reflected intensity at the bottom of minerals, it can be used to compare the mineral content relative to the same type of mineral in other samples (Okawara et al., 1996).

## 2.2. Leaching Test

Leaching test was performed with sample A, B, C and D so as to understand the acid generating potential of the samples. After sieving the samples into 1.5-2.0 mm, they were packed into a glass column (40.4 mm diameter × 58.9 mm height). 10 mm thickness of a supporting layer was installed by setting paper filter, 0.5-1.0 mm of glass beads, and sieves at the bottom of the column to support the samples. In order to unify the reactive area of the samples in each column, the porosity was calculated using the density of the samples and the volume of filling the samples and set at 60%. 100 ml of distilled water was poured into the column and the leachate was sampled from the



bottom of the column for the measurement of pH, followed by the drying process by using an artificial light for 24 hours. The weight of the samples after pouring distilled water was confirmed to decrease to the initial weight of the samples at the end of the drying process. After the wetting and drying cycle was repeated until 10 times, 14 days of the drying process was prepared without an artificial light. The step of 10 times of the wetting and drying cycle with 14 days of the drying process was, furthermore, repeated until 3 times. The total number of the supply of 100 ml of distilled water was 30 times in this study on the assumption of annual rainfall in the mine area in Indonesia. Thus, the wetting and drying cycle was attributed to the supply of distilled water and the heat of the artificial light in this experiment. Additionally, 20.6% of O<sub>2</sub> was measured with oxygen meter (Toray, LC-450F, Japan) at the top and the bottom of the column at the end of every drying process, indicating that same amount of oxygen was supplied to the samples in each column during the drying process. At the end of the leaching test, grain size analysis was, besides, conducted so that the progress of the weathering of rocks with the occurrence of AMD during the leaching test was examined.

### 2.3. Slaking Index (SI) Test to Understand Physical Weathering of Rocks

Slaking of rocks which is caused by the swelling pressure of clay minerals through the wetting and drying cycle is classified into physical weathering of rocks (Karathanasis et al., 2014). In this study, Slaking Index (SI) test was performed to understand the slaking behavior of the rock samples (Sadisun et al., 2003). Less than 2 mm of the samples was removed by sieving and the weight of more than 2 mm of the samples was measured after the wetting and drying cycle in SI test. SI was calculated as the indicator of slaking using the change of the weight of the samples until 5 times.

### 2.4. Acid Extraction Test to Understand Chemical Weathering of Rocks

Acid extraction test was carried out by reference to the analysis conducted by Sasaki et al. (2002) to elucidate the form of sulfur and iron in the rock samples since the dissolution rate of elements depends on the form of minerals (Sasaki et al., 2002).

Minerals can be extracted with acids at each stage of the extraction (Huerta-Diaz and Morse, 1990). 2.5 g of dried sample was dissolved with 20 ml of 1 mol/dm<sup>3</sup> hydrochloric acid (HCl), 60 ml of 46% hydrogen fluoride (HF), and 10 ml of conc. nitric acid (HNO<sub>3</sub>) in line with the method in the past research (Sasaki et al., 2002). Sasaki et al. (2002) mentioned that soluble minerals were extracted with HCl, and

silicate minerals were extracted with HF, and refractory minerals such as sulfide minerals were extracted with HNO<sub>3</sub>. In this study, the time of shaking of the mixture at HNO<sub>3</sub> step was changed from 2 hours in the past research to 6 hours in order to dissolve sulfide minerals completely. The proportion of each form of sulfur and iron composing pyrite was calculated based on the amount of extracted sulfur and iron (mg/g) from rock samples.

## **2.5. Simple Dissolution Test and Scanning Electron Microscopy (SEM)**

### **Observation**

Simple dissolution test was conducted by reference to the standard of the pH<sub>1:2</sub> test of AMIRA in addition to the acid extraction test so as to observe the chemical weathering of rocks: the ratio of solid to liquid was 1:2 (AMIRA, 2002). The size of samples was changed from -75 µm in the standard to 1.0 mm in order to clearly observe the change of surface conditions of the samples before and after the simple dissolution test using Scanning Electron Microscopy (SEM). The sample which underwent the wetting and drying cycle was used to compare the amount of extracted iron and sulfur with HCl in the acid extraction test and the amount of dissolved sulfur and iron in the leachate in the simple dissolution test. The leachate was supplied to Inductively Coupled

Plasma-Atomic Emission Spectrometry (ICP-AES) to measure the concentration of sulfur and iron soon after the simple dissolution test in order not to accelerate the reaction of the samples with oxygen and water. The results were calculated using the unit of mg/g to compare the results of the simple dissolution test and the acid extraction test. Besides, the samples after the simple dissolution test were dried by lyophilizer filled with nitrogen gas to prevent the oxidation of the samples before the observation using SEM. The progress of chemical weathering of rocks was investigated based on the change of surface conditions of the rock samples before and after the simple dissolution test.

### 3. RESULTS AND DISCUSSION

In order to clarify each experiment and the purpose, the experimental scheme is presented in Table 1.

**Table 1.**

### 3.1. Acid Generating Potential of Rock Samples

The XRD patterns of the rock samples are shown in Figure 1. The peaks of quartz and kaolinite were found in all samples. The peaks of pyrite were clearly observed in sample B and D, indicating that the content of pyrite was high in sample B and D. The peaks of albite were clearly seen in only sample A, B, and C, while it was not found in sample D. Additionally, only sample A contained siderite based on the result in Figure 1. Table 2 shows QI which was calculated using the intensity of each mineral in Figure 1, and Figure 2 shows the chemical component of the samples: others in sample B and D were mostly composed of water. Although QI of quartz was quite low in sample D, similar values of QI of kaolinite were obtained in all samples. Besides, QI of albite was slightly higher in sample C. The content of silica in each sample in Figure 2 was supported by QI of quartz in Table 2. Moreover, a large amount of iron and sulfur in sample B and D in Figure 2 was well correlated with the peaks of pyrite in the samples in Figure 1. Pyrite was not observed in sample A and C in Figure 1; however, the sulfur content was 0.83% and 0.03% in sample A and C, respectively. This suggested that sample A and C may contain small amount of sulfide causing AMD.

215

216

217

**Fig. 1.**

218

219

220

**Table 2.**

221

222

223

**Fig. 2.**

224

225

226 Figure 3 shows the change of pH in the leaching test. The change of pH can be

227 classified into two groups. The pH in sample B and D remained at pH 2.0-3.0, while

228 sample C showed a rapid increase in pH at the early step of leaching, followed by a

229 gradual increase at pH 7.0-8.0. Furthermore, sample A showed a gradual increase in pH

230 overall. As the content of pyrite was high in sample B and D, the pH in sample B and D

231 remained at low-pH with the dissolution of pyrite in the leaching test. On the other hand,

232 the pH gradually increased in sample A and C because of the low content of sulfur.

233 During the drying process in the leaching test, the same amount of oxygen was supplied  
234 to the samples: 20.6% of oxygen was measured with oxygen meter at the top and the  
235 bottom of the column at the end of drying process. In sample B and D in which the  
236 content of pyrite was high, acidic water, therefore, occurred at the rate comparable to  
237 the amount of oxygen supply, resulting in similar pH at each step of leaching.  
238 Meanwhile, sample A and C showed a gradual increase in pH since only residual sulfide  
239 caused acidic water by reacting with the oxygen supply at each step of leaching. The  
240 decrease of the amount of sulfide in sample A and C with the step of leaching resulted  
241 in the gradual increase in pH. Thus, it was found that the change of pH was dependent  
242 on the sulfur content in rocks and the amount of oxygen supply. There was, moreover, a  
243 sharp drop in pH after 14 days of the drying process in all samples, especially in sample  
244 A, B, and D, as indicated by means of arrows in Figure 3. This suggested that the  
245 amount of oxygen supply during the drying process played an important role in the  
246 progress of AMD. Consequently, the wetting and drying cycle attributed to the supply  
247 of deionized water and the heat of the artificial light accelerated the deterioration in the  
248 water quality with the dissolution of sulfide in the leaching test. The sulfur content in  
249 rocks and the amount of oxygen supply, especially, played an important role in the  
250 change of pH on the basis of the results in this study.

**Fig. 3.**

### **3.2. Physical Weathering of Rocks**

The change of slaking index (SI) of the samples is displayed in Figure 4. The particle size distribution after the leaching test is described in Figure 5. There was a rapid increase in SI at the first step in sample A, B, and C, followed by a slight increase until the fifth step, whereas SI gradually increased overall in sample D in Figure 4. This result indicated that sample A, B, and C easily disintegrated through the wetting and drying cycle, which is called as a rapid slaking (Tanaka et al., 1997). In contrast, sample D gradually disintegrated through the wetting and drying cycle. The particle size of the rock samples in the columns was set at 1.5-2.0 mm before beginning the leaching test as shown by a straight line in Figure 5. More than 50% of the rock samples consisted of less than 0.25 mm of small particles in sample A, B, and C after the leaching test as indicated by a circle in Figure 5. The rate of decline of particle size was consistent with the change of slaking index in Figure 4, indicating that rapid slaking caused a



significant decrease of particle size in sample A, B, and C through the wetting and drying cycle during the leaching test. However, the particle size of approximately 30% of sample A was more than 1 mm after the leaching test, while that of more than 90% of sample B, C, and D were less than 1 mm. This was attributed to the prevention of slaking in sample A due to the compacted layer formed in the surface layer as shown in Figure 6. Approximately 1 mm of small particles were observed under the compacted layer at the end of the leaching test in sample A. For these results, the compacted layer prevented the progress of slaking in sample A, leading to the middle size of the residue in the column after the leaching test. Although some of the particles in sample A were not slaked owing to the compacted layer, the decrease of particle size after the leaching test was observed in all samples.

In general, clay minerals cause the disintegration of rocks by slaking with swelling pressure while swelling and shrinking with the wetting and drying cycle (Karathanasis et al., 2014). This is considered physical weathering of rocks since the swelling pressure causes the disintegration of rocks. The clay minerals which have a large specific surface area compared with other clay minerals, such as kaolinite, montmorillonite, and illite, significantly contribute to the progress of slaking (Pusch, 1983; Ruiz-Vera and Wu, 2006; Emerson, 1964). In regard to the facts and the result of XRD, kaolinite caused

disintegration of rocks by slaking through the wetting and drying cycle in this study.

Albite also causes slaking of rocks through the hydrolysis of albite according to the past research, but it is very minor effect (Wen et al., 2014). Other clay minerals causing slaking were not observed in all samples in this study. Therefore, the disintegration of rocks by physical weathering was mainly caused by kaolinite during the leaching test and SI test. In spite of the similar content of kaolinite in all samples, the change of SI of sample D in Figure 4, however, differed from that of the other samples, indicating that the change of SI was affected by other factors in this study. Additionally, the disintegration of rocks can accelerate AMD through the increase of the reactive area of rocks, but the pH remained at low-pH overall in sample B and D with the wetting and drying cycle in Figure 3 even if the rock samples disintegrated due to physical weathering during the leaching test. This also suggested that the change of pH depended on the sulfur content and the amount of oxygen supply more than the effect of physical weathering of rocks.

**Fig. 4.**

**Fig. 5.**

**Fig. 6.**

### **3.3. Chemical Weathering of Rocks**

The proportion of the extracted sulfur and iron in the acid extraction test is described by each step of the extraction in Figure 7. The solubility of the elements depends on the existing form of minerals in rocks: sulfate, generally, dissolve in leachate more easily than sulfide (Turkdogan et al., 1974). Thereby, the minerals extracted with HCl affect the water quality in a short time for the high solubility compared with that with HNO<sub>3</sub>, whereas the minerals extracted with HNO<sub>3</sub> contribute to the water quality for a long time owing to the low solubility. In Figure 7, iron and sulfur existed in different form of minerals in the rock samples according to the results: minerals extracted at HCl step, at HF step, and at HNO<sub>3</sub> step. Considering that sulfate can be extracted with HCl and

sulfide can be extracted with  $\text{HNO}_3$  in the acid extraction test, more than 81% of sulfur and iron existed as sulfide in sample D, and approximately 35% of iron and 60% of sulfur were extracted as sulfide in sample B. Since the high content of sulfide in sample B and D caused acidic water for a long term, the pH remained at low-pH overall in sample B and D in Figure 3. Approximately 0-12% of iron and 42-50% of sulfur were extracted as sulfide, and the sulfur content was 0.83% and 0.03% in sample A and C, respectively. The ratio of sulfate was, moreover, higher in sample A and C than that in sample B and D. Hence, most of the soluble sulfates dissolved in the leachate at the early stage of leaching in sample A and C, leading to a gradual increase of pH in Figure 3. It can, furthermore, be seen that high content of siderite resulted in the highest ratio of iron extracted with  $\text{HCl}$  in sample A. In short, the existence form of sulfur and iron in rocks played an important role in the change of the water quality: this result was consistent with that of the previous study (Matsumoto et al., 2015).

Figure 8 shows the comparison between the amount of extracted iron and sulfur with  $\text{HCl}$  and  $\text{HNO}_3$  before and after the wetting and drying cycle. While the amount of extracted iron and sulfur with  $\text{HNO}_3$  was higher before the wetting and drying cycle, that with  $\text{HCl}$  was higher after the wetting and drying cycle in the figure. In terms of the formation of precipitation and/or sulfate with the occurrence of AMD, they were formed

341 from sulfide during the wetting and drying cycle and dissolved by HCl. Thus, soluble

342 minerals are formed with the occurrence of AMD during the wetting and drying cycle.

343 The amount of sulfur and iron extracted with HCl after the wetting and drying cycle  
344 is compared with the amount of dissolved sulfur and iron in the leachate in the simple  
345 dissolution test in Figure 9. It suggested that soluble sulfate extracted with HCl was

346 easily dissolved in leachate when they were exposed to water. The amount of dissolved

347 elements was not in good agreement with the amount of extracted iron and sulfur with

348 HCl in sample A and C; however, similar values were obtained in sample B and D.

349 Considering the small amount of sulfur and iron content in sample A and C in Figure 2,

350 the difference was attributed to the heterogeneous distribution of sulfur and iron in

351 rocks. Consequently, the elements which were extracted with HCl easily dissolved in

352 the leachate, leading to AMD in a short time.

353  
354  
355 **Fig. 7.**

**Fig. 8.**

**Fig. 9.**

Figure 10 shows the surface conditions of the rock samples after the wetting and drying cycle and the simple dissolution test. While the products which are thought of as oxidative products and/or precipitations were observed on the surface of the samples after the wetting and drying cycle in Figures 10a<sub>1</sub>, b<sub>1</sub>, c<sub>1</sub>, and d<sub>1</sub>, they were not observed after the simple dissolution test in Figures 10a<sub>2</sub>, b<sub>2</sub>, c<sub>2</sub>, and d<sub>2</sub>. The changes were clearly observed in sample B and D which contained a large amount of iron and sulfur compared to that in sample A and C. In addition, micro-cracks were observed on the surface of the rock samples after the simple dissolution test as presented by white circles in Figure 10a<sub>3</sub>, b<sub>3</sub>, c<sub>3</sub>, and d<sub>3</sub>. Considering that the elements extracted with HCl dissolved in the simple dissolution test, the micro-cracks were developed at the voids

which were formed after the dissolution of soluble minerals. According to the previous research, the dissolution of soluble minerals can lead to the decrease of the strength of rocks (Tran et al., 2011; Ciantia et al., 2015). The strength decreased and the micro-cracks occurred as the result of the formation of void after the dissolution of soluble minerals. This phenomenon was considered chemical weathering of rocks in this study since the dissolution of soluble sulfur and iron led to the development of micro-cracks on the surface of rocks. Therefore, chemical weathering of rocks and the occurrence of AMD progressed simultaneously through the wetting and drying cycle with the acidification of rocks. Although the chemical weathering caused by dissolution of soluble iron and sulfur occurred in the leaching test, it can be said that the change of pH was mainly affected by sulfur content, the existence form of sulfur and iron in rocks, and the amount of oxygen supply more than the effect of the chemical weathering in this study.

**Fig. 10.**

### 3.4. Interaction of Physical Weathering and Chemical Weathering of Rocks

On the basis of the results as shown above, chemical and physical weathering of rocks progressed simultaneously with the occurrence of AMD during the wetting and drying cycle in the argillaceous rocks which contained sulfide and clay minerals related to slaking. In view of the fact that the physical weathering of rocks causes cracks by swelling of clay minerals and the chemical weathering causes micro-cracks with the dissolution of soluble sulfur and iron, physical weathering can be accelerated by chemical weathering with the development of cracks from micro-cracks as shown in Figure 11. Physical weathering of rocks by slaking due to swelling of kaolinite and the hydrolysis of albite and chemical weathering with micro-cracks on the surface of rocks caused by the dissolution of soluble sulfur and iron occurred with the progress of AMD during the leaching test and SI test in this study. Given that the proportion of soluble iron and sulfur in sample A, B, and C was higher than that in sample D by approximately 30% in the ratio, the occurrence of the micro-cracks on the surface of rocks with the dissolution of soluble sulfur and iron significantly accelerated the disintegration of rocks caused by slaking of kaolinite, resulting in the rapid increase of SI in sample A, B, and C in SI test in spite of the similar amount of kaolinite in all samples. It was, however, found that the sulfur content, the existence form of sulfur and



iron in rocks, and the amount of oxygen supply significantly affected the change of the water quality although the physical and chemical weathering of rocks could affect the progress of AMD with the increase of specific surface area through disintegration of rocks.

**Fig. 11.**

#### **4. CONCLUSIONS**

The interaction between physical and chemical weathering of rocks as well as the effect of the interaction on AMD were investigated by performing the leaching test, slaking index (SI) test, and acid extraction test with sample analysis before and after the wetting and drying cycle. The conclusions are summarized as follows:

- I. The argillaceous rock which contained sulfide caused chemical weathering with micro-cracks on the surface of rocks through the dissolution of soluble iron and sulfur along with the occurrence of AMD.

II. The chemical and physical weathering of rocks by swelling of clay minerals progressed simultaneously with the wetting and drying cycle. Furthermore, chemical weathering accelerated physical weathering of rocks with the occurrence of micro-cracks on the surface of rocks after the dissolution of soluble sulfur and iron.

III. Although the disintegration of rocks by physical and chemical weathering could affect the progress of AMD, the change of the water quality by AMD over time was significantly affected by the amount of oxygen supply, the sulfur content, and the existence form of sulfur and iron in rocks more than the effect of rock weathering.

**ACKNOWLEDGEMENTS:** The authors would like to express their gratitude and appreciation to the mine for providing the rock samples in this study. We are also grateful to engineers in the mine and colleagues in Kyushu University for supporting the part of the sampling and the analysis.

## REFERENCES

- AMIRA International, 2002, ARD test handbook: prediction & kinetic control of acid mine drainage, AMIRA P387A. Reported by Ian Wark Research Institute and Environmental Geochemistry International Ltd. Melbourne, Australia, AMIRA International.
- Ciantia, O.M., Castellanza, R., Crosta, B.G., and Hueckel, T., 2015, Effects of mineral suspension and dissolution on strength and compressibility of soft carbonate rocks. *Engineering Geology*, 184, 1–18.
- Dold, B., Toril, G.E., Aguilera, A., Pamo, L.E., Cisternas, E.M., Bucchi, F., and Amils, R., 2013, Acid rock drainage and rock weathering in Antarctica: important sources for iron cycling in the southern ocean. *Environmental Science and Technology*, 47, 6129–6136.
- Emerson, W.W., 1964, The slaking of soil crumbs as influenced by clay mineral composition. *Australian Journal of Soil Research*, 2, 211–217.
- Huerta-Diaz, A.M. and Morse, W.J., 1990, Quantitative method for determination of trace metal concentration in sedimentary pyrite. *Marine Chemistry*, 29, 119–144.

464 Jennings, S.R., Neuman, D.R., and Blicher, P.S., 2008, Acid Mine Drainage and Effects  
 465 on Fish Health and Ecology: a Review. Reclamation Research Group Publication,  
 466 Bozeman, 26 p.

467 Karathanasis, D.A., Murdock, W.L., Matocha, J.C., Grove, J., and Thompson, L.Y.,  
 468 2014, Fragipan horizon fragmentation in slaking experiments with amendment  
 469 materials and ryegrass root tissue extracts. The Scientific World Journal, 2014, 1–  
 470 13.

471 Lobb, D. and Femmer, S., 2007, Missouri streams fact sheet: watersheds. In: Wolken, S.  
 472 (ed.), Missouri Stream Team. Missouri Conservation Department, Jefferson, 1–13.

473 Matsumoto, S., Ishimatsu, H., Shimada, H., Sasaoka, T., Matsui, K., Kusuma, J.G.,  
 474 2015, Prevention of acid mine drainage (AMD) by using sulfur-bearing rocks for a  
 475 cover layer in a dry cover system in view of the form of sulfur. Journal of the  
 476 Polish Mineral Engineering Society, 36, 29-35.

477 Moon, V. and Jayawardane, J., 2004, Geomechanical and geochemical changes during  
 478 early stages of weathering of Karamu basalt, New Zealand. Engineering Geology,  
 479 74, 57–72.

480 Okawara, M., Yoneda, T., Mitachi, T., and Tada, M., 1996, Mineralogical/chemical  
 481 evaluation of shear zone clay for paleo–slip surface determination – A case study

482        in the Myoukurasawa paleo-landslide area, Iwate prefecture -. Journal of the Japan  
 483        Society of Engineering Geology, 37, 2-13.

484        Pusch, R., 1983, Use of clays as buffers in radioactive repositories. Technical Report  
 485        83-46, University of Lulea, Division of Soil Mechanics, Lulea, 86 p.

486        Ruiz-Vera, M.V., and Wu, L., 2006, Influence of sodicity, clay mineralogy, prewetting  
 487        rate, and their interaction on aggregate stability. Soil Science Society of America  
 488        Journal, 70, 1825-1833.

489        Sadisun, A.I., Shimada, H., Ichinose, M., and Matsui, K., 2003, Further developments  
 490        in procedures to determine durability characteristics of argillaceous rocks using a  
 491        static slaking index test. Proceedings of the 1<sup>st</sup> International Workshop on Earth  
 492        Science and Technology, Fukuoka, November 7, p. 179-186.

493        Sasaki, K., Haga, T., Hirajima, T., and Kurosawa, K., 2002, Distribution and transition  
 494        of heavy metals in mine tailing dumps. Materials Transactions, 43, 2778-2783.

495        Wen, B., Li, H., Ke, K., 2014, Effect of soaking on shear strength of weathered  
 496        argillaceous rocks susceptible to landsliding in the three gorges area of China. In:  
 497        Sassa, K. et al. (ed.), Landslide Science for a Safer Geoenvironment, Vol. 2.  
 498        Springer International Publishing Switzerland 2014, 135-140.

Tanaka, U., Yokoi, Y., Kosaki, T., and Kyuma, K., 1997, Mechanisms and processes of crust formation on artificial aggregates: effect of slaking and impact of rain drops on crusting under different moisture conditions. Soil Science and Plant Nutrition, 43, 109–115.

Tran, K.M., Shin, H., Byun, Y., and Lee, J., 2011, Mineral dissolution effects on mechanical strength. Engineering Geology, 125, 26–34.

Turkdogan, T.E., Rice, B.B., Vinters, V.J., 1974, Sulfide and sulfate solid solubility in lime, magnesia, and calcined dolomite: part I. CaS and CaSO<sub>4</sub> solubility in CaO. Metallurgical Transactions, 5, 1527-1535.

## Figure Captions

**Table 1.** Summary of experiment and the purpose in this study.

**Table 2.** Quartz Index (QI) calculated based on the intensity in the result of XRD,

**Fig. 1.** X-ray diffraction (XRD) patterns of sample A, B, C, and D. Qz, Ka, Al, Si, and Py represent quartz, kaolinite, albite, siderite, and pyrite, respectively.

**Fig. 2.** Chemical composition of sample A, B, C, and D.

**Fig. 3.** Change of pH in sample A, B, C, and D in the leaching test.

**Fig. 4.** Change of slaking index (SI) in sample A, B, C, and D.

**Fig. 5.** Change of particle size distribution before and after the leaching test: initial size of the samples was set at 1.5-2.0 mm.

**Fig. 6.** Physical conditions of sample A after the leaching test. (a) Physical conditions of the surface layer in the column from side view. (b) Middle-size particles under the compacted layer after the leaching test from top view.

**Fig. 7.** Proportion of extracted iron and sulfur at each step of the acid extraction. (a) Proportion of extracted iron. (b) Proportion of extracted sulfur.

**Fig. 8.** Comparison of the amount of extracted iron and sulfur with HCl and HNO<sub>3</sub> before and after the wetting and drying cycle. (a) Comparison of the amount of extracted iron. (b) Comparison of the amount of extracted sulfur.

**Fig. 9.** Comparison of the amount of extracted iron and sulfur with HCl in the acid extraction test and that of dissolved iron and sulfur in the simple dissolution test. (a) Comparison of the amount of soluble iron. (b) Comparison of the amount of soluble sulfur.

**Fig. 10.** Surface conditions of sample A, B, C, and D. Symbol of “a, b, c, d” represents sample A, B, C, and D, respectively. (1) After the wetting and drying cycle. (2) After

534 the simple dissolution test. (3) Micro-crack on the surface of rocks after the simple  
535 dissolution test.

536 **Fig. 11.** Interaction between physical and chemical weathering of rocks.